THE ASTROPHYSICAL JOURNAL, 485:359–369, 1997 August 10


# ULTRAVIOLET AND OPTICAL OBSERVATIONS OF HEN 1213, HEN 1341, AND HEN 1761

A. GUTIÉRREZ-MORENO, H. MORENO,[1] AND E. COSTA[1]
Departamento de Astronomía, Universidad de Chile, Casilla 36-D, Santiago, Chile;
agutierr@das.uchile.cl, hmoreno@das.uchile.cl, ecosta@das.uchile.cl

AND

W. A. FEIBELMAN[2]
Laboratory for Astronomy and Solar Physics, Code 681, NASA Goddard Space Flight Center, Greenbelt, MD 20771;
feibelman@stars.gsfc.nasa.gov

*Received 1996 November 1; accepted 1997 March 14*

## ABSTRACT

We present UV observations of the symbiotic stars Hen 1213, Hen 1341, and Hen 1761, made almost simultaneously with optical observations during 1995; previous optical observations were made during 1987 and 1991. The UV spectrum of Hen 1213 was badly affected by background radiation, and only a rough description of the spectrum could be given here; for this reason, only the observations of Hen 1341 and Hen 1761 are discussed. They have the typical spectra of symbiotic stars, with a late giant component, with many emission lines superimposed. It is found that for both objects the reddening determined from He II $\lambda$1640/ He II $\lambda$4686 is smaller than that obtained from the Balmer decrement, including optical depth effects. Hen 1341 does not show important variations for the three observing periods. Hen 1761 shows P Cygni profiles for He II $\lambda$4686 and He I $\lambda$4471, with expansion velocities of the order of 900 and 600 km $s^{-1}$, respectively. The 1991 observations give the lower temperature of the hot component with the larger size of the nebula and the lowest He contents. Rough estimates indicate that the hot component of Hen 1761 is smaller and less luminous than that of Hen 1341.

*Subject headings:* binaries: symbiotic — stars: individual (Hen 1213, Hen 1341, Hen 1761) — ultraviolet: stars

## 1. INTRODUCTION

Hen 1213 ($\alpha = 16^h35^m15^s.2$, $\delta = -51°42'24''$[2000.0]), Hen 1341 ($\alpha = 17^h08^m36^s.7$, $\delta = -17°26'29''$ [2000.0]), and Hen 1761 ($\alpha = 19^h42^m25^s.9$, $\delta = -68°07'41''$ [2000.0]) are symbiotic S-type stars for which few observations have been presented in the literature.

In his Catalogue of Symbiotic Stars, Allen (1984) lists these stars as having no known optical variations; orbital periods are not mentioned. The spectra presented, obtained in 1977 and 1978, are not calibrated in flux. Hen 1341 clearly shows the 6830 Å band (identified by Schmid 1989 as due to Raman scattering by neutral H of the O VI resonance ultraviolet doublet), which indicates a high temperature of the hot source. This band is not present in Hen 1213 and Hen 1761.

In the *IRAS* Point Source Catalog, Version 2 (1988) we found the following fluxes in janskys for Hen 1761: 12 $\mu$m, 0.42; 25 $\mu$m, 0.27 (lower limit); 60 $\mu$m, 0.40 (lower limit); 100 $\mu$m, 1.26 (lower limit). No data are given for Hen 1213 or Hen 1341.

Near-infrared magnitudes and colors are presented in Table 1, where the first line of each color corresponds to the data given by Allen (1982) and the second line to those given by Munari et al. (1992). The values presented by these two authors show only minor variations.

We made visual spectroscopic observations of these three objects during 1987 and 1991, gathering a large amount of information. In 1995 we observed these stars in both the UV and optical regions of the spectrum. We report here the results of the previous and the new observations.

## 2. THE ULTRAVIOLET OBSERVATIONS

### 2.1. *Observations*

The three symbiotic stars were observed for the first time in the low-resolution ($\delta\lambda \approx 7$ Å) mode of the *IUE* as summarized in the log of observations in Table 2. All exposures were made through the large ($10'' \times 23''$) entrance aperture of the SWP and LWP cameras and were centered on the star. Target acquisitions were made by offsets from bright SAO stars. The *IUE* observations were planned to coincide, or nearly coincide, with ground-based observations from CTIO. Observations of Hen 1341 were affected by background radiation, and those for Hen 1213 were severely affected by an extraordinarily high radiation level (200 DN), but Hen 1761 was observed under very good conditions. We show the observed emission-line fluxes for Hen 1341 and Hen 1761 in Table 3. For Hen 1213 we can only state that lines of C IV, He II, and C III] are present, but their flux measurements are very unreliable.

### 2.2. *Data Analysis*

The *IUE* data were reduced at the Goddard Data Analysis Center (IUEDAC) by the use of the standard interactive computer routines available to guest observers. Emission-line fluxes were measured by the routine FEATURE that also gives the wavelength of the centroids of an emission feature. The fluxes are accurate to $\pm 15\%$ for

[1] Visiting Astronomer, Cerro Tololo Inter-American Observatory, National Optical Astronomy Observatories, operated by the Association of Universities for Research in Astronomy, Inc. (AURA), under cooperative agreement with the National Science Foundation.

[2] Guest Observer with the *International Ultraviolet Explorer* (*IUE*) satellite, which is sponsored and operated by the National Aeronautics and Space Administration, by the European Space Agency, and by the Science and Engineering Research Council of the United Kingdom.

TABLE 1

INFRARED COLORS

| Parameter | Hen 1213 | Hen 1341 | Hen 1761 |
|---|---|---|---|
| $K$ | 6.72 | 7.58 | 5.55 |
| | ... | 7.66 | 5.58 |
| $J-H$ | 1.08 | 0.98 | 1.10 |
| | ... | 1.06 | 1.05 |
| $H-K$ | 0.29 | 0.34 | 0.17 |
| | ... | 0.31 | 0.28 |
| $K-L$ | ... | ... | 0.17 |
| | ... | ... | 0.17 |
| $K-L'$ | 0.19 | ... | ... |
| | ... | ... | ... |
| Spectral type | K4 | M0 | M3 |

well-exposed features, and the wavelengths have been rounded off to two significant figures. Line-by-line analysis shows that all spectra were well centered on the echelle lines 55 and 56 in the large entrance apertures of the *IUE* cameras. The spectra are presented in Figures 1 and 2.

### 2.3. *Description of the Spectra*

The *IUE* spectra of Hen 1761 and Hen 1341 are typical of those observed for symbiotic stars. The strongest emission in Hen 1761 is C IV, while for Hen 1341 it is He II. For Hen 1761, six pixels of the emission line C IV $\lambda$1549 are saturated, as are a few pixels for He II $\lambda$1640 in Hen 1341. These are not thought to affect the flux measurement by more than a few percent and are within the nominal $\pm$15% accuracy of the *IUE* spectra. None of the other features is saturated. The N V doublet at 1240 Å may have a P Cygni profile for both objects. The SWP spectrum for Hen 1761 is of very high quality and possibly shows a P Cygni profile for He II $\lambda$1640. A much smaller absorption appears to be present for He II $\lambda$1640 in the Hen 1341 data. In the atlas of *IUE* low-dispersion SWP spectra for 32 symbiotic stars by Meier et al. (1994), the C IV $\lambda$1549 emission is usually the strongest feature by far, except for five objects that show He II $\lambda$1640 as the strongest emission.

Recent LWP spectra are sometimes contaminated by scattered sunlight that causes a "streak," resulting in a false

TABLE 2

LOG OF UV OBSERVATIONS

| Object | Date 1995 | Spectrum | Exposure Time (minutes) | Comments |
|---|---|---|---|---|
| Hen 1341 | Apr 12 | SWP 54402 | 40 | High radiation |
| Hen 1341 | Apr 12 | LWP 30434 | 20 | High radiation |
| Hen 1213 | Apr 12 | SWP 54403 | 20 | 200 DN radiation |
| Hen 1213 | Apr 12 | LWP 30435 | 15 | 200 DN radiation |
| Hen 1761 | Apr 19 | SWP 54467 | 20 | C IV 6 pixels saturated |
| Hen 1761 | Apr 19 | LWP 30483 | 20 | Slight "streak" |

TABLE 3

OBSERVED UV EMISSION-LINE FLUXES FOR HEN 1341 AND HEN 1761

| $\lambda$(obs) (Å) | | $\lambda$(lab) | | FLUX[a] | | |
|---|---|---|---|---|---|---|
| Hen 1341 (1) | Hen 1761 (2) | Å (3) | ION (4) | Hen 1341 (5) | Hen 1761 (6) | COMMENTS (7) |
| 1239.50 | 1237.44 | 1238, 1242 | N V | 13.2 | 31.4 | Doublet |
| 1301.78 | ... | 1301, 1304 | O I | 6.3 | ... | Doublet |
| 1400.88 | 1400.19 | 1393, 1402 | Si IV, O IV | 15.7 | 32.3 | Blended |
| 1485.18 | 1483.49 | 1483, 1486 | N IV | 5.6 | 3.2 | Doublet |
| 1545.83 | 1547.02 | 1548, 1550 | C IV | 38.9 | 204.7 | Doublet |
| 1573.30 | 1574.87 | 1574.8 | [Ne V] | 1.7: | 4.5 | |
| ... | 1598.61 | 1601.6 | [Ne IV] | ... | 4.6 | |
| 1638.53 | 1638.54 | 1640.4 | He II | 42.3 | 33.1 | P Cygni? |
| 1661.50 | 1662.96 | 1661, 1665 | O III] | 14.8 | 30.4 | Doublet |
| 1700.11 | 1701.54 | 1702.0 | Fe II? | 4.0 | 1.9: | P Cygni? |
| ... | 1712.74 | 1718.5 | N IV] | ... | 2.8 | |
| 1747.60 | 1749.38 | 1746, 1752 | N III] | 4.2 | 3.9 | Multiplet |
| ... | 1810.03 | 1814.7 | [Ne III] | ... | 2.3 | Broad |
| 1887.18 | ... | 1888.9 | Si I? | 1.2: | ... | |
| 1896.18 | 1890.43 | 1892.0 | Si III] | 2.3 | 2.7 | Blended in |
| 1906.49 | 1908.51 | 1907, 1909 | C III] | 7.2 | 15.2 | Hen 1341 |
| ... | 2251.39 | 2252.0 | Ne V? | ? | 7.8 | |
| ... | 2424.14 | 2421.8 | [Ne IV] | ... | 1.4: | Doublet |
| 2840.44 | 2835.53 | 2836.3 | O III | 4.4 | 3.2 | Bowen |
| ... | 2892.39 | 2888.1 | Fe II? | ... | 2.1: | |
| ... | 3024.77 | 3024.7 | O III | ... | >0.5: | Bowen |
| ... | 3049.68 | 3047.1 | O III | ... | >0.6: | Bowen |
| 3133.70 | 3137.79 | 3132.9 | O III | >14.3 | >7.2 | On "streak" |

NOTE.—A colon means that the line is very weak; $\pm$30% error.

[a] In units of $10^{-13}$ ergs cm$^{-2}$s$^{-1}$:

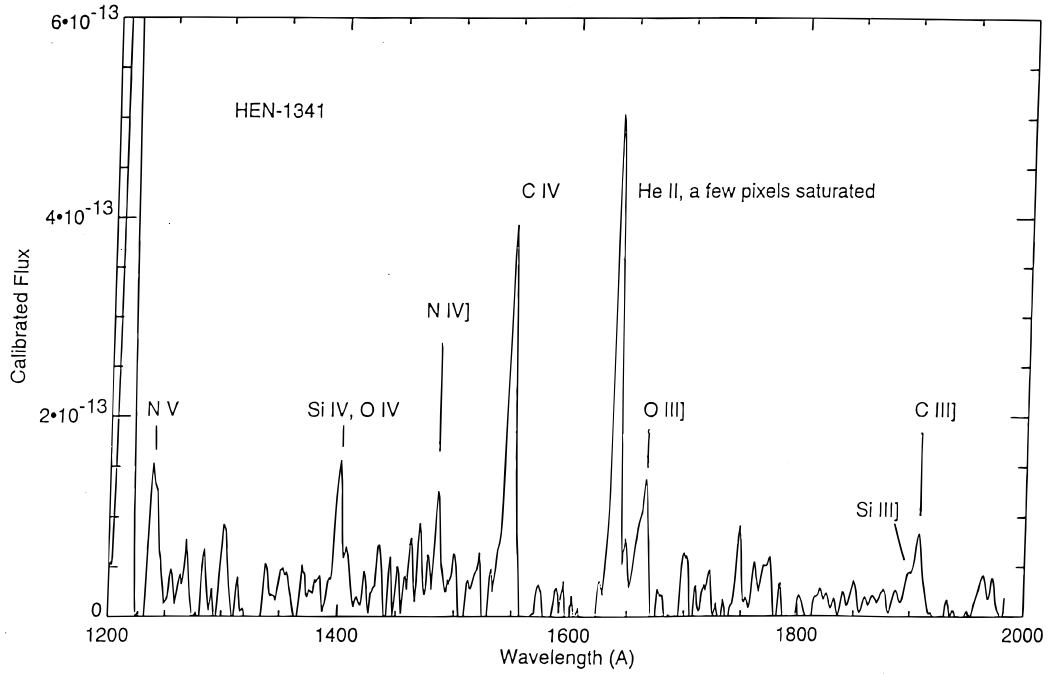


FIG. 1.—Ultraviolet spectrum of the symbiotic star Hen 1341, showing the region 1200–2000 Å. This is a low-dispersion exposure (SWP 54402) of 40 minute duration. Some emission features are identified.

rise of the continuum toward longer wavelengths. Thus, the LWP spectra may be of limited value shortward of 2800 Å. We detected a weak [Ne IV] λ2424 doublet for Hen 1761. The strongest feature in the LWP spectra of both objects is the O III Bowen line at 3133 Å, accompanied by weak signatures of the λλ2836, 3025, 3047 Bowen series.

## 3. OPTICAL OBSERVATIONS

### 3.1. *Observations*

Details of the observations of Hen 1341 and Hen 1761 are given in Table 4, which lists (1) the name of the objects; (2) the date of the observations; (3) and (4) telescopes and

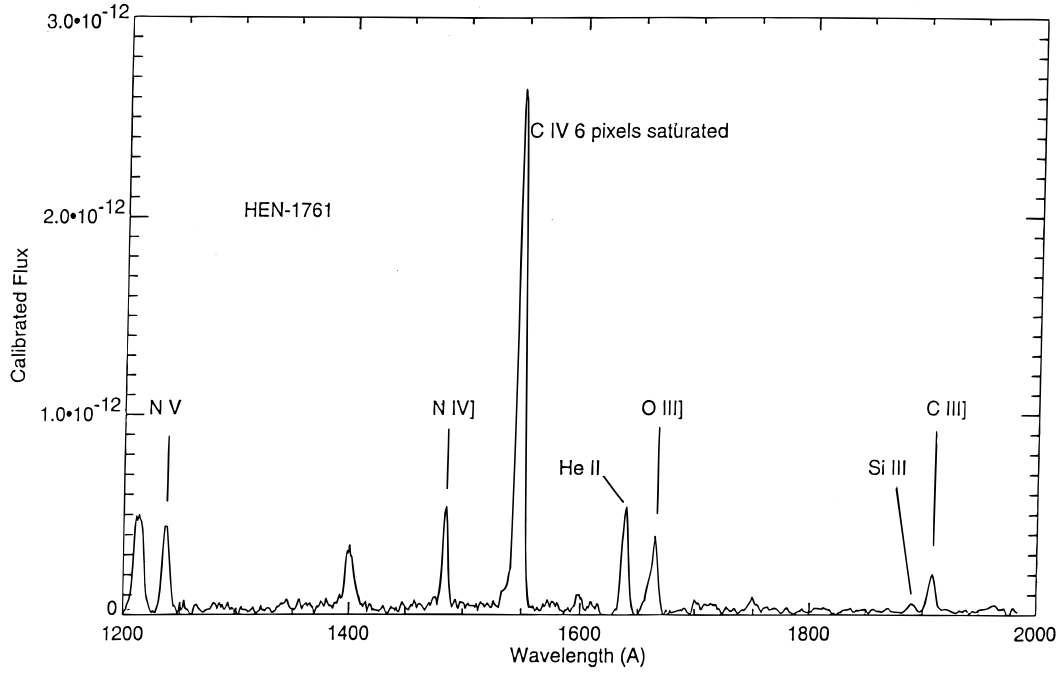


FIG. 2.—Ultraviolet spectrum of the symbiotic star Hen 1761, showing the region 1200-2000 Å. This is a low-dispersion exposure (SWP 54467) of 20 minute duration. Some emission features are identified. The line He II λ1640 may have a P Cygni profile, while the C IV λ1549 unresolved resonance doublet has a weak wing on its shortward side.

TABLE 4

LOG OF OPTICAL OBSERVATIONS

| Name | Date | Telescope | Detector | Slit Width (arcsec) | Wavelength Range (Å) | FWHM (Å) | Exposure Time (s) | Filter | N |
|---|---|---|---|---|---|---|---|---|---|
| Hen 1341..... | 1987 Jul 04 | 1.0 m | 2D-F | 10 | 3800–7200 | 5 | 600 | WG 360 | 2 |
| | 1987 Jul 06 | 1.0 m | 2D-F | 10 | 3800–7200 | 5 | 600 | WG 360 | 1 |
| | 1991 Jun 29 | 1.0 m | 2D-F | 5 | 3300–6700 | 5 | 1800 | ... | 2 |
| | 1991 Jul 06 | 1.5 m | GEC CCD | 3 | 3100–7700 | 17 | 350 | ... | 2 |
| | 1991 Jul 06 | 1.5 m | GEC CCD | 10 | 3100–7700 | 17 | 100 | ... | 1 |
| | 1991 Jul 10 | 1.5 m | GEC CCD | 3 | 6300–10700 | 16 | 500 | RG 610 | 1 |
| | 1991 Jul 10 | 1.5 m | GEC CCD | 10 | 6300–10700 | 16 | 100 | RG 610 | 1 |
| | 1995 Apr 10 | 1.5 m | GEC CCD | 3 | 4600–7100 | 9 | 60 | GG 455 | 2 |
| | 1995 Apr 10 | 1.5 m | GEC CCD | 10 | 4600–7100 | 9 | 60 | GG 455 | 3 |
| | 1995 Apr 12 | 1.5 m | GEC CCD | 3 | 4000–5400 | 5 | 240 | ... | 3 |
| | 1995 Apr 12 | 1.5 m | GEC CCD | 10 | 4000–5400 | 5 | 240 | ... | 2 |
| Hen 1761..... | 1987 Jul 03 | 1.0 m | 2D-F | 10 | 3800–7200 | 5 | 900 | WG 360 | 2 |
| | 1987 Jul 03 | 1.0 m | 2D-F | 10 | 3800–7200 | 5 | 900 | WG 360 | 2 |
| | 1987 Jul 03 | 1.0 m | 2D-F | 10 | 3800–7200 | 5 | 900 | WG 360 | 1 |
| | 1991 Jun 30 | 1.0 m | 2D-F | 5 | 3400–6800 | 5 | 1800 | ... | 1 |
| | 1991 Jul 01 | 1.0 m | 2D-F | 5 | 4400–7700 | 5 | 1800 | GG 455 | 1 |
| | 1995 Apr 10 | 1.5 m | GEC CCD | 3 | 4600–7100 | 9 | 240 | GG 455 | 3 |
| | 1995 Apr 10 | 1.5 m | GEC CCD | 10 | 4600–7100 | 9 | 180 | GG 455 | 2 |
| | 1995 Apr 12 | 1.5 m | GEC CCD | 3 | 4000–5400 | 5 | 900 | ... | 2 |
| | 1995 Apr 12 | 1.5 m | GEC CCD | 10 | 4000–5400 | 5 | 500 | ... | 3 |

detectors used; (5) slit width in arcseconds; (6) wavelength range in angstroms; (7) resolution (FWHM) in angstroms; (8) exposure time in seconds; (9) blocking filter used (if any); and (10) the number of spectra obtained with each setup. For all the observations the slit was oriented in the east-west direction. Some objects were observed both through a narrow slit (3″ or 5″) to obtain the best spectral resolution, and through a wide slit ($\approx$10″) to obtain accurate spectrophotometry. The standard stars were taken from Stone & Baldwin (1983) for the 2D-FRUTTI (2D-F) observations, from Taylor (1984) for the 1991 CCD observations, and from Stone & Baldwin (1983) as improved by Hamuy et al. (1992) for the 1995 CCD observations. The standard stars were always observed with the wide slit. Hen 1213 was also observed, but because of the problems presented by the UV observations, we will discuss it in another paper.

### 3.2. *Data Reductions*

The data reductions were performed at the CTIO La Serena Computing Center. All the observations were reduced to linear wavelength and flux scales using IRAF.[3] The spectra thus obtained were then measured using the task SPLOT in IRAF at the Centro de Procesamiento Digital de Imágenes (CPDI) of the Departamento de Astronomía de la Universidad de Chile; the blends were resolved using the DEBLEND option in the task SPLOT. All the spectra obtained through a narrow slit were reduced to the wide spectra without losing resolution. The fluxes measured for the emission lines are listed in Table 5, which gives, separately, the results of the measures for each epoch of observation. Typical errors of the measures are in the range of about 5%–10% for lines with $\log F(\lambda) > -12$ to about 60% for $\log F(\lambda) \leq -15$.

[3] IRAF is distributed by National Optical Astronomy Observatories, which are operated by the Association of Universities for Research in Astronomy, Inc., under contract to the National Science Foundation.

### 3.3. *Description of the Spectra*

The optical spectra of Hen 1341 and Hen 1761 are shown in Figures 3 and 4. These spectra are typical of symbiotic stars in the red, with strong absorption bands of TiO. The spectra are rich in emission lines and molecular bands. The Balmer continuum is strongly in emission, which supports the presence of a considerable contribution to the continuum from gas recombination processes. The Balmer series is clearly seen in the spectra corresponding to 1991.

Except for the variation of H$\alpha$, the spectrum of Hen 1341 shows rather minor changes from 1987 to 1995, so we have represented in Figure 3 only the combined spectrum corresponding to 1991 July, which includes a wavelength range from $\approx$3000 to 10200 Å. This spectrum allowed us to measure up to H12 ($\lambda$3752), while those obtained in June, with better resolution, show clearly up to H16 ($\lambda$3704). The Paschen series is also seen; its lines could, however, be blended with molecular lines. Bowen fluorescence lines at 3133, 3340, and 3444 Å are visible in the blue in the 1991 July spectrum; the line at 3133 Å is fainter than that observed in 1995 in the UV. The 6830 Å band is clearly present, but $\lambda$7088 is not detected.

One of the strongest features in the near-infrared is the emission line [O I] $\lambda$8664, corresponding to the transition $3\ ^3S^o$–$3\ ^3P$, which is observed in emission in Be stars and in novae (Andrillat 1982). Its intensity is much higher than that of [O I] $\lambda$7772. No hint of a P Cygni profile is seen in He II $\lambda$4686 or in other lines.

The spectra of Hen 1761 are quite different for the different epochs of observation; for this reason we have represented in Figure 4 the three spectra, with a separation step of $4 \times 10^{-13}$ ergs cm$^{-2}$ s$^{-1}$. Especially noticeable is the difference in the ratio [O III] $\lambda$4363/H$\gamma$.

Only the line at 3444 Å of the Bowen fluorescence series was observed. The 6830 Å band is not present.

In the three spectra the lines He II $\lambda$4686 and He I $\lambda$4471 show P Cygni profiles, although they are much more noticeable in the 1995 spectra. In the three cases the profiles

TABLE 5

MEASURED FLUXES ($H\beta$ + He II Pi8 = 100)

| $\lambda$ (Å) | Ion | Hen 1341 | | | Hen 1761 | | | Comments |
|---|---|---|---|---|---|---|---|---|
| | | 1987 | 1991 | 1995 | 1987 | 1991 | 1995 | |
| 3133 ..... | O III | ... | 17.4 | ... | ... | ... | ... | Bowen |
| 3203 ..... | He II | ... | 14.6 | ... | ... | ... | ... | |
| 3344 ..... | [Ne III] + [Ne V] | ... | 11.4 | ... | ... | 2.87 | ... | |
| 3426 ..... | [Ne V] | ... | 17.0 | ... | ... | ... | ... | |
| 3444 ..... | O III | ... | 11.6 | ... | ... | 6.27 | ... | Bowen |
| 3704 ..... | H16 | ... | 1.91 | ... | ... | ... | | |
| 3710 ..... | H15 | ... | 0.71 | ... | ... | ... | ... | |
| 3722 ..... | H14 | ... | 1.89 | ... | ... | ... | ... | |
| 3734 ..... | H13 | ... | 1.73 | ... | ... | 1.07 | ... | |
| 3752 ..... | H12 | ... | 4.08 | ... | ... | 5.03 | ... | |
| 3771 ..... | H11 | ... | 3.44 | ... | ... | 3.16 | ... | |
| 3798 ..... | H10 | ... | 2.91 | ... | ... | 5.32 | ... | |
| 3835 ..... | H9 | 5.42 | 5.81 | ... | 9.79 | 5.97 | ... | |
| 3869 ..... | [Ne III] + He I | 5.86 | 5.90 | ... | 29.4 | 6.60 | ... | |
| 3889 ..... | He I + H8 | 11.1 | 9.15 | ... | 19.3 | 10.5 | ... | |
| 3969 ..... | [Ne III] + He II + H7 | 13.8 | 12.9 | ... | 21.9 | 15.3 | ... | |
| 4026 ..... | He I + He II | 1.81 | 1.77 | 1.71 | 3.34 | ... | 15.0 | |
| 4072 ..... | [S II] | 1.79 | 1.86 | 2.66 | 5.27 | 1.56 | 4.50 | Doublet |
| 4101 ..... | $H\delta$ + He II | 18.5 | 18.0 | 13.2 | 24.3 | 19.3 | 22.4 | |
| 4340 ..... | $H\gamma$ | 34.7 | 33.0 | 31.5 | 45.4 | 36.7 | 39.4 | |
| 4363 ..... | [O III] | 5.69 | 9.22 | 6.70 | 27.7 | 10.8 | 21.8 | |
| 4388 ..... | He I | 2.43 | 3.10 | 3.35 | 3.87 | 4.61 | 2.29 | |
| 4472 ..... | He I | 3.22 | 4.03 | 4.10 | 5.65 | 2.51 | 5.98 | P Cygni |
| 4542 ..... | He II | 2.26 | ... | 2.39 | ... | ... | ... | |
| 4641 ..... | N III | 3.09 | 8.90 | 5.25 | ... | ... | ... | |
| 4686 ..... | He II | 44.2 | 42.6 | 50.9 | 38.4 | 8.97 | 43.8 | P Cygni |
| 4861 ..... | $H\beta$ | 100 | 100 | 100 | 100 | 100 | 100 | |
| 4922 ..... | He I | 8.00 | 8.29 | 9.88 | 15.8 | 6.38 | 4.52 | |
| 4959 ..... | [O III] | 11.0 | 11.1 | 12.5 | ... | ... | ... | |
| 5007 ..... | [O III] | 43.1 | 35.9 | 37.9 | 40.8 | 13.1 | 44.5 | |
| 5016 ..... | He I | 9.03 | 7.09 | 5.35 | ... | 5.70 | 6.04 | |
| 5412 ..... | He II | 4.95 | 5.12 | 3.81 | ... | ... | ... | |
| 5755 ..... | [N II] | ... | ... | ... | ... | ... | 17.8 | |
| 5876 ..... | He I | 22.3 | 24.0 | 23.0 | 36.5 | 17.0 | 56.7 | |
| 6087 ..... | [Ca V] + [Fe VII] | 3.59 | 2.75 | 2.63 | ... | ... | ... | |
| 6563 ..... | $H\alpha$ | 867 | 585 | 620 | 727 | 483 | 475 | |
| 6678 ..... | He I | 22.1 | 19.3 | 22.1 | 35.6 | 9.59 | 44.3 | |
| 6830 ..... | O VI | 23.5 | 17.3 | 25.5 | ... | ... | ... | Raman? |
| 7065 ..... | He I | 20.7 | 17.8 | ... | 29.7 | 14.3 | ... | |
| 7772 ..... | O I | ... | 3.15 | ... | ... | ... | ... | |
| 8446 ..... | O I | ... | 36.6 | ... | ... | ... | ... | |
| 8503 ..... | H I (P16) | ... | 6.44 | ... | ... | ... | ... | |
| 8545 ..... | H I (P15) | ... | 7.24 | ... | ... | ... | ... | |
| 8598 ..... | H I (P14) | ... | 5.96 | ... | ... | ... | ... | |
| 8665 ..... | H I (P13) | ... | 5.65 | ... | ... | ... | ... | |
| 8751 ..... | H I (P12) | ... | 7.07 | ... | ... | ... | ... | |
| 8863 ..... | H I (P11) | ... | 7.53 | ... | ... | ... | ... | |
| 9015 ..... | H I (P10) | ... | 6.53 | ... | ... | ... | ... | |
| 9229 ..... | H I (P9) | ... | 8.14 | ... | ... | ... | ... | |
| 9546 ..... | H I (P8) | ... | 8.52 | ... | ... | ... | ... | |
| 10050..... | H I (P7) | ... | 21.1 | ... | ... | ... | ... | |
| 10124..... | He II | ... | 20.6 | ... | ... | ... | ... | |

correspond to expansion velocities of $\approx 900 \pm 100$ and $600 \pm 100$ km s$^{-1}$, respectively.

The behavior of the different lines is analyzed in Figures 5*a*–5*c*, which represent the observed absolute fluxes for (*a*) the H lines, (*b*) the He I lines, and (*c*) He II $\lambda$4686 plus some forbidden lines; only the lines with observations during the three epochs have been represented. The graphs show that almost all the lines have a maximum intensity in 1991; the exceptions are He I $\lambda$6678, He II $\lambda$4686, and [S II] $\lambda$4072, for which, in any case, the observed absolute fluxes are more intense in 1991 than in 1995.

## 4. THE LATE COMPONENT

### 4.1. *Spectral Types of the Late Components*

The spectral types of the late components were obtained by the $[TiO]_1$, $[TiO]_2$, and [VO] indices given by Kenyon & Fernández-Castro (1987) and by the [TiO] index given by Kenyon (1986); they were determined separately for each period of observations. The latest spectral type obtained for each object was adopted, because of the possibility that the absorption bands are being veiled in some cases by the nebular component. The final spectral type adopted was

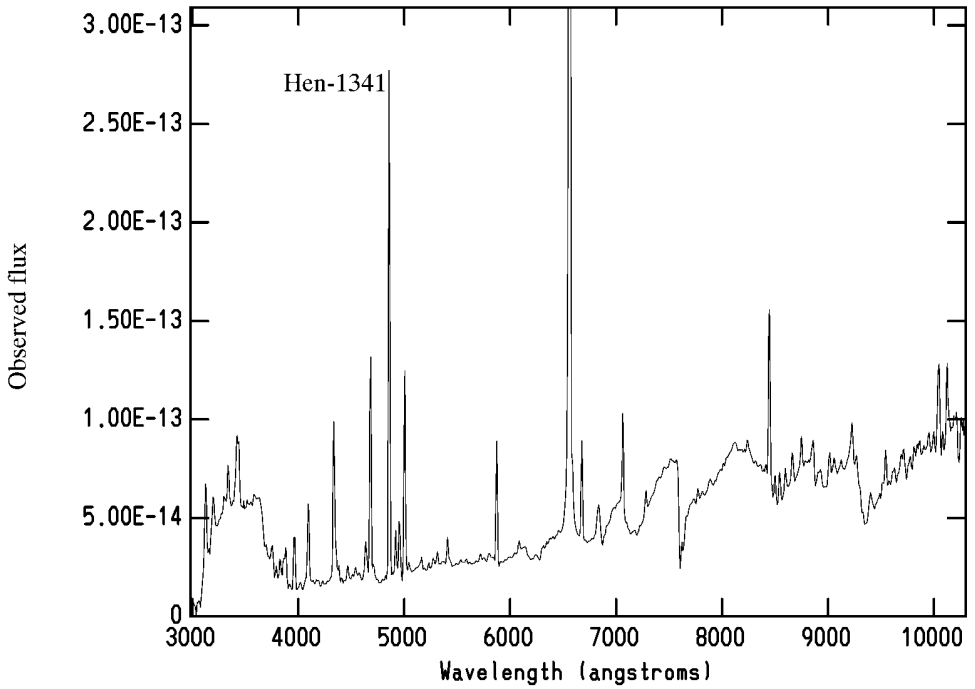


FIG. 3.—Combined CCD optical spectrum of Hen 1341 obtained in 1991 July, showing the region 3100–10200 Å. The Balmer discontinuity is seen strongly in emission. Absorption bands are noticeable. The band at 6830 Å is rather wide. [O I] $\lambda$8664 is very strong.

confirmed by visual comparison with the digital spectra published by Turnshek et al. (1985).

### 4.2. *Absolute Magnitudes and Distances*

Assuming that all the flux in the $K$ band corresponds only to the late giant, for the determination of the absolute $K$ magnitudes we used the spectral types obtained in § 4.1 and the relevant data for M-type giants taken from Tsuji (1978) and from Dyck, Lockwood, & Capps (1974). The distance was then estimated from the distance moduli by using these absolute magnitudes, the value of $A_K$, and the observed magnitudes listed by Allen (1982).

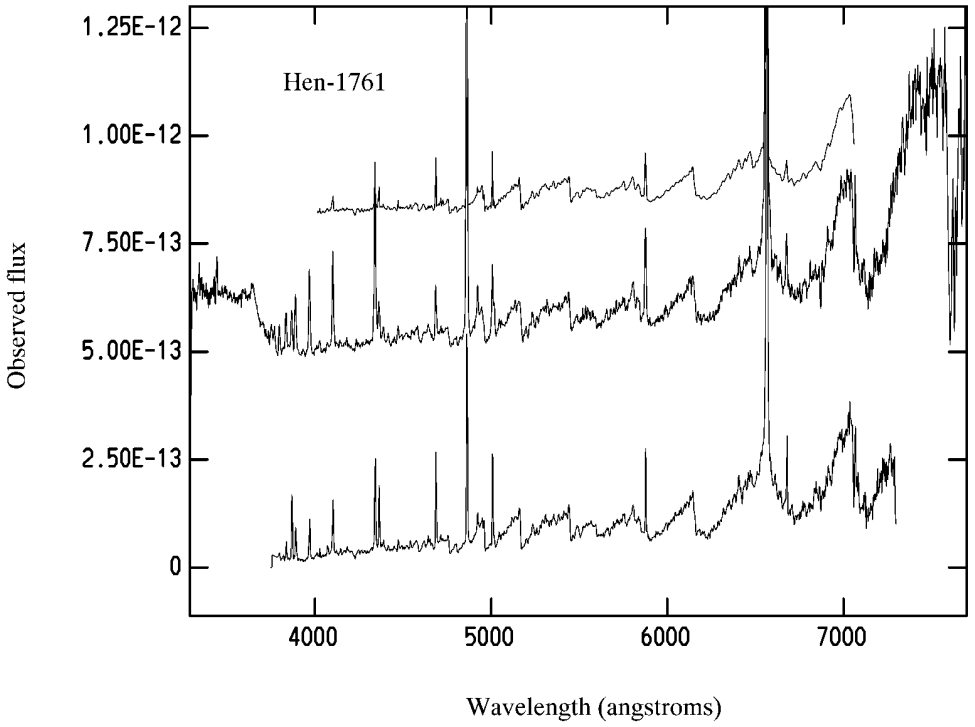


FIG. 4.—Spectra of Hen 1761, showing from bottom to top the spectra corresponding to 1987, 1991, and 1995. The zero points of the three spectra are located at 0, $4.00 \times 10^{-13}$, and $8.00 \times 10^{-13}$, respectively. The variation of the intensities of the lines is clearly appreciated. Notice that H$\beta$ in 1991 reaches the top of the figure, while in 1995 it is much smaller.

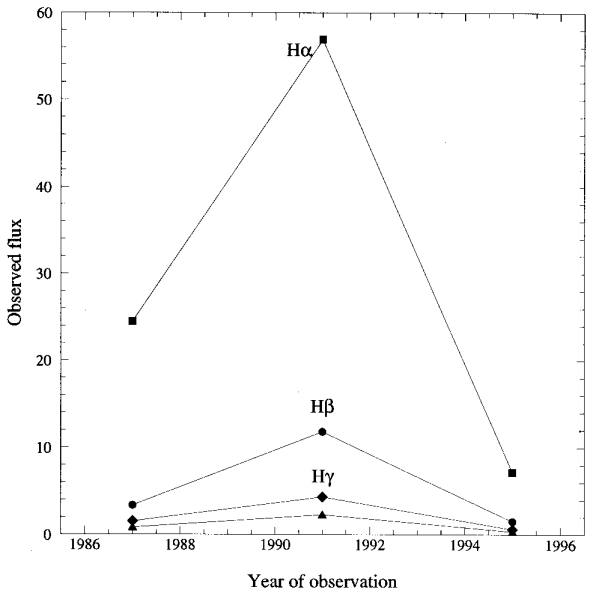


FIG. 5a

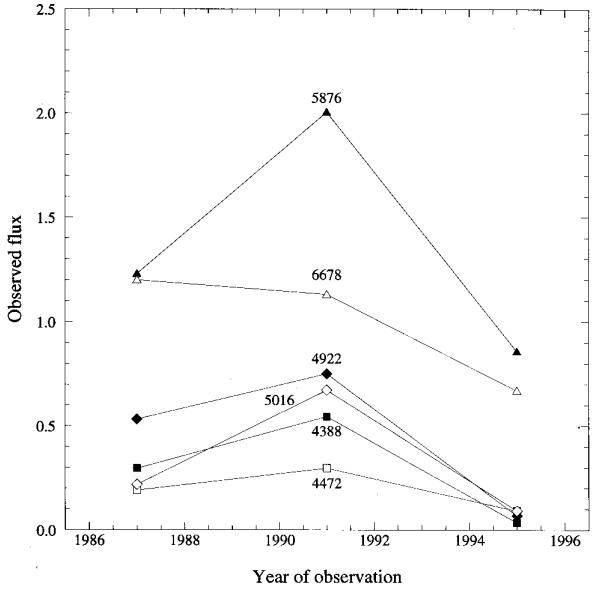


FIG. 5b

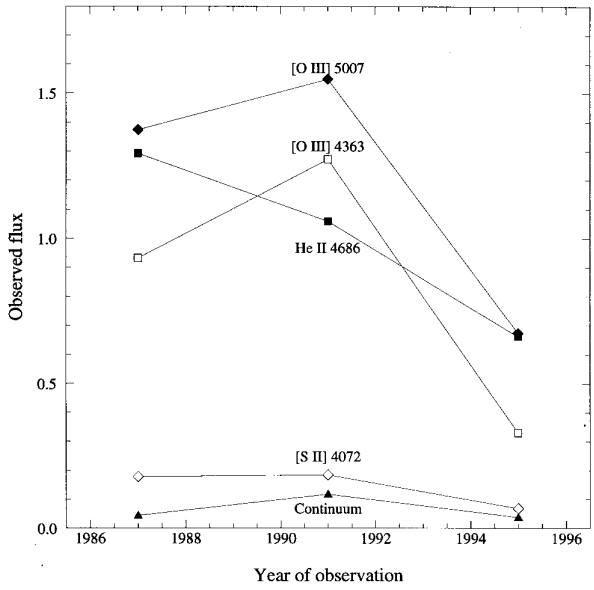


FIG. 5c

FIG. 5.—Variation with time of the intensity of different features of the spectrum (ordinates are in units of $10^{-12}$ ergs cm$^{-2}$ s$^{-1}$). (*a*) H lines; the line below H$\gamma$ corresponds to H$\delta$. (*b*) He I lines. (*c*) He II $\lambda$4686 and some forbidden lines; the line below [S II] represents the continuum, taken at each date as the average of $\lambda\lambda$4686, 4861, 5007; in this case the units are $10^{-12}$ ergs cm$^{-2}$ s$^{-1}$Å$^{-1}$. Notice that the continuum corresponding to 1991 was obtained through a narrow slit, so that the point represented here corresponds to a minimum value.

## 5. THE NEBULAR COMPONENT

### 5.1. *Reddening and Optical Depth*

The determination of the reddening constants $C\beta$ in the visual region of the spectrum, and of the optical depths at H$\alpha$, $\tau$(H$\alpha$), with their standard errors (which reflect mainly the good agreement between the observations of the different Balmer lines), was made using the procedure described by Gutiérrez-Moreno & Moreno (1996) using Seaton's (1979) reddening curve. The emissivities at different optical depths as listed by Netzer (1975) for $N_e = 10^9$ were used for all the determinations. In one case (Hen 1341, 1991 observations) we have several lines of the Paschen series and the corresponding lines of the Balmer series. Assuming that there are not self-absorption effects, as shown by the value $\tau$(H$\alpha$) = 0, and using the ratios Pa$n$/H$n$, with $n$ = 9–15, we could also obtain a value of $C\beta$. Besides, we obtained an estimate of the reddening by means of the infrared photometry published by Allen (1984) and by Munari et al. (1992); from their data we obtained the observed $(J-K)$ colors and compared them with Johnson's (1966) standard colors corresponding to the spectral types determined in the preceding paragraph, obtaining $E(J-K)$ and then using the interstellar absorption curve of Savage & Mathis (1979), $E(B-V)$. The value thus derived assumes that all the radiation in the $J$ and $K$ bands comes from the late component, and that this component has not suffered any major variations with time. The reddenings obtained from all these methods are fairly consistent.

The reddening constants were also obtained for the 1995

observations by using the ratio of the He II lines in the UV and optical wavelengths, $F(\lambda 1640)/F(\lambda 4686)$ (Feibelman 1982). For both objects we found large differences between these $E(B-V)$ values and those obtained by the preceding methods. Further considerations, which will be explained in the next paragraph, led us to accept the Balmer decrement value of $C\beta$ as the most adequate for these observations. From the reddening constant adopted we deduced the reddening $E(B-V)$ and from it the total absorption at $V$ and $K$, $A_V = 3.2E(B-V)$ and $A_K = 0.38E(B-V)$.

### 5.2. *Absolute Hβ Intensity*

To obtain the absolute H$\beta$ intensity, the observed flux must be corrected by the reddening determined in the preceding subsection, in addition to a correction for self-absorption. This last correction was determined assuming that all the H$\beta$ radiation comes from the nebula, without contribution from the core, and applying the numerical procedure suggested as a good first approximation by Ahern (1975).

### 5.3. *Plasma Diagnostic*

We determined the electron density from the ratio of the observed UV fluxes $F$(Si III]) /$F$(C III]) for both objects by the use of the diagnostic curves of Feibelman & Aller (1987). These lines are well resolved for Hen 1761 but are blended for Hen 1341.

From the optical observations, we have determined the temperature corresponding to the high-density limit ($N_e \geq 10^9$ cm$^{-3}$), from the [O III] ratio $I(\lambda 5007 + \lambda 4959)/I(\lambda 4363)$, where $I$ represents reddening-corrected fluxes; estimates of the corresponding densities have also been obtained. For the 1995 observations we have obtained $T_e$ and $N_e$ by means of the Nussbaumer & Storey (1981) diagnostic diagram. This determination was made using the $C\beta$ values deduced from the optical data and from the UV-optical data. For both objects, the logarithm of the density derived when using the UV-optical reddening constants is somewhat smaller than that obtained from the UV $F$(Si III])/$F$(C III]) ratio, which is independent of reddening; but the values obtained from the optical reddenings are in excellent agreement with the UV values. Because of this agreement we adopted in what follows the optical values of $C\beta$. The temperatures indicated by the Nussbaumer & Storey (1981) diagram are practically identical to the high-density limiting temperature.

### 5.4. *Helium Abundances*

The He abundance was determined using the He I emissivities given by Almog & Netzer (1989) for $4 < \log N_e < 14$ and $T_e = 10^4$ K. In general, the lines used were He I $\lambda\lambda$3889, 4471, 5876, and 7065. The emissivities listed by Almog & Netzer (1989) for different densities were used to interpolate the values for $\log N_e = 11$. Besides, we have interpolated the emissivities for the temperatures determined in the preceding paragraph by means of an expression of the form

$$E(t) = E(1)t^{\gamma} ,$$

where $t = T_e \times 10^{-4}$, $E(t)$ is the emissivity for a given temperature, and $\gamma$ was obtained from the Almog & Netzer (1989) values for $N_e = 10^{10}$ cm$^{-3}$ and $T_e = 10{,}000$ and 20,000 K. The value of $\gamma$ was determined for each of the wavelengths used and for each value of $\tau(\lambda 3889)$; it was assumed that the values thus obtained are applicable to all the values of $N_e$. The line He I $\lambda$6678 was not used, since in general Almog & Netzer (1989) do not give its emissivity. When the value of $\tau$(H$\alpha$) obtained in § 5.1 is greater than unity, we have used H$\gamma$ as the reference line, since the higher the order of the line, the smaller the self-absorption effects. For the 1995 observations, where $\lambda$7065 was not observed, we adopted for $\tau(\lambda 3889)$ the values derived from the previous observations.

### 5.5. *Nebular Radius*

According to Kenyon (1986), the electron densities derived from UV data may be combined with the flux of H$\beta$ to estimate the nebular radius if the distance is known. Assuming constant density through the nebula and case B recombination, the nebular radius in astronomical units is given approximately by

$$R_{\rm neb} \approx 0.3 d^{2/3} n_9^{-2/3} I(\mathrm{H}\beta)^{1/3} ,$$

where $d$ is the distance in kpc, $n_9$ is the electron density in units of $10^9$ cm$^{-3}$, and $I$(H$\beta$) is the H$\beta$ intensity corrected for reddening and self-absorption and expressed in units of $10^{-12}$ ergs cm$^{-2}$ s$^{-1}$. The results obtained are only reasonable estimates, since symbiotic stars do not have constant-density nebulae, and case B recombination does not apply to these objects.

All the parameters obtained from § 4 and this section are presented in Table 6, which lists, for each object and epoch of observation, (1) the observed value of log $F$(H$\beta$), corrected by the contamination of He II Pi8; (2) the reddening constant $C\beta$; (3) the optical depth at H$\alpha$ derived from the Balmer decrement considering self-absorption effects [the value of $C\beta$ in item 2 will be used when pertinent in what follows; for the 1995 observations of Hen 1341, a negative value of $\tau$(H$\alpha$) was obtained, and $\tau$(H$\alpha$) = 0 was adopted]; (4) the coefficient $C_s$, which corrects $I$(H$\beta$) for self-absorption; the value $C_s = 1.0$ was adopted for $\tau$(H$\alpha$) = 0 for Hen 1341 in 1991; (5) the logarithm of the intensity of H$\beta$, corrected for reddening and self-absorption; (6) the reddening constant as obtained from the Balmer and Paschen series when the latter is available; (7) the reddening $E(B-V) = C\beta/1.47$, obtained from item 2; (8) the reddening $E(B-V)$ as obtained from the infrared colors; the values obtained from Allen (1982) colors are listed in 1987, while the values obtained from Munari et al. (1992) colors are listed in 1991 and 1995; (9) the value of $E(B-V)$ as obtained from the He II ratio $F(\lambda 1640)/F(\lambda 4686)$; (10) the visual absorption $A_V = 3.2E(B-V)$; (11) the absorption for the $K$ magnitude, $A_K = 0.38E(B-V)$; (12) the $K$ magnitude as given by Allen (1984); (13) the value of $T_e$ corresponding to the high-density limit; (14) an estimate of the electron density for a temperature close to the limiting temperature just given; (15) the logarithm of the density obtained for 1995 from the $F$(Si III])/$F$(C III]) ratio; (16) and (17) the logarithm of the electron density and the electron temperature obtained from the Nussbaumer & Storey (1981) diagnostic diagram; (18) the logarithm of the nebular radius expressed in centimeters; (19) the weighted mean of the abundance $y^+ = N(\mathrm{He\ II})/N(\mathrm{H}^+)$ with weights proportional to the observed fluxes of the lines used in the determination; (20) the abundance $y^{++} = N(\mathrm{He\ III})/N(\mathrm{H}^+)$; since $y^{++}$ was derived from only one line, the error quoted in this case corresponds to the error of the mean flux of the line $\lambda$4686 as measured in each period of observation; (21) the total He contents, $y = y^+ + y^{++} = N(\mathrm{He})/N(\mathrm{H})$; (22) the spectral

TABLE 6

PARAMETERS

| PARAMETER | HEN 1341 | | | HEN 1761 | | |
|---|---|---|---|---|---|---|
| | 1987 | 1991 | 1995 | 1987 | 1991 | 1995 |
| 1. log $F(H\beta)$ | $-11.40 \pm 0.01$ | $-11.38 \pm 0.02$ | $-11.42 \pm 0.01$ | $-11.47 \pm 0.02$ | $-10.93 \pm 0.01$ | $-11.82 \pm 0.03$ |
| 2. $C\beta$ | $1.21 \pm 0.05$ | $1.07 \pm 0.10$ | $1.34 \pm 0.07$ | $0.66 \pm 0.04$ | $0.83 \pm 0.04$ | $0.62 \pm 0.08$ |
| 3. $\tau(H\alpha)$ | $2.7 \pm 0.5$ | $0.0 \pm 0.6$ | 0 | $6.3 \pm 0.6$ | $0.0 \pm 0.2$ | $1.0 \pm 0.6$ |
| 4. $C_s$ | $1.28 \pm 0.07$ | $1.01 \pm 0.07$ | 1.00 | $1.56 \pm 0.09$ | $1.00 \pm 0.05$ | $1.12 \pm 0.09$ |
| 5. log $I(H\beta)$s | $-10.08 \pm 0.08$ | $-10.31 \pm 0.14$ | $-10.08 \pm 0.08$ | $-10.62 \pm 0.07$ | $-10.10 \pm 0.08$ | $-11.15 \pm 0.13$ |
| 6. $C\beta$(Paschen-Balmer) | ... | $1.35 \pm 0.23$ | ... | ... | ... | ... |
| 7. $E(B-V)$(Balmer) | 0.82 | 0.73 | 0.91 | 0.45 | 0.56 | 0.42 |
| 8. $E(B-V)$(IR) | 0.61 | 0.71 | 0.71 | 0.51 | 0.63 | 0.63 |
| 9. $E(B-V)$(UV) | ... | ... | $0.29 \pm 0.07$ | ... | ... | $0.08 \pm 0.04$ |
| 10. $A_V$ | 2.62 | 2.33 | 2.91 | 1.44 | 1.79 | 1.34 |
| 11. $A_K$ | 0.37 | 0.28 | 0.35 | 0.17 | 0.21 | 0.16 |
| 12. $K$ | 7.58 | 7.58 | 7.58 | 5.55 | 5.55 | 5.55 |
| 13. $T_e$(lim) | $7200 \pm 9\%$ | $8300 \pm 10\%$ | $7700 \pm 10\%$ | $10400 \pm 7\%$ | $11300 \pm 9\%$ | $9400 \pm 8\%$ |
| 14. log $N_e$(visual) | 10.1 | 10.5 | ... | 10.0 | 10.1 | ... |
| 15. log $N_e$(UV) | ... | ... | $11 \pm 0.2$ | ... | ... | $10 \pm 0.1$ |
| 16. log $N_e$(NS) | ... | ... | $10.8 \pm 0.2$ | ... | ... | $9.6 \pm 0.1$ |
| 17. $T_e$(NS) | ... | ... | $7600 \pm 7\%$ | ... | ... | $9350 \pm 4\%$ |
| 18. log $R$(neb) | $11.9 \pm 0.2$ | $10.9 \pm 0.2$ | $10.1 \pm 0.2$ | $11.7 \pm 0.1$ | $12.1 \pm 0.2$ | $11.2 \pm 0.1$ |
| 19. $y^+$ | $0.077 \pm 0.005$ | $0.063 \pm 0.005$ | $0.071 \pm 0.004$ | $0.095 \pm 0.008$ | $0.062 \pm 0.001$ | $0.190 \pm 0.025$ |
| 20. $y^{++}$ | $0.091 \pm 0.015$ | $0.081 \pm 0.012$ | $0.102 \pm 0.015$ | $0.048 \pm 0.008$ | $0.013 \pm 0.003$ | $0.028 \pm 0.004$ |
| 21. $y$ | $0.168 \pm 0.015$ | $0.144 \pm 0.013$ | $0.173 \pm 0.016$ | $0.143 \pm 0.011$ | $0.075 \pm 0.003$ | $0.218 \pm 0.025$ |
| 22. S.T. | M1.7 $\pm$ 0.4 | M1.7 $\pm$ 0.2 | M1.2 $\pm$ 0.5 | M5.1 $\pm$ 0.3 | M3.4 $\pm$ 0.8 | M4.9 $\pm$ 0.3 |
| 23. Adopted | | M1.7 $\pm$ 0.3 | | | M5.0 $\pm$ 0.3 | |
| 24. $M_K$ | | $-5.21 \pm 0.11$ | | | $-7.46 \pm 0.19$ | |
| 25. Distance (kpc) | | $3.08 \pm 4\%$ | | | $3.71 \pm 8\%$ | |

types of the late components corresponding to each period; (23) the adopted spectral type for each object; (24) the determined absolute $K$ magnitude; and (25) the distance in kiloparsecs (the errors quoted in this case include only the effect of the errors in the absolute magnitudes due to the errors in the spectral types. No errors are listed in line 14 of the table, since the values quoted for the electron density are only estimates for arbitrarily adopted temperatures.

## 6. THE HOT SOURCE

### 6.1. *Temperature of the Hot Sources*

We have estimated the upper and lower limits for the radiation temperature of the hot sources. We first determined the temperature from Iijima (1981), who uses the intensity of the lines He II $\lambda$4686 and He I $\lambda$4471. If we assume that the nebula is particle bounded, the flux in H$\beta$ will be more reduced by self-absorption than the flux in He II. The temperature thus obtained will then be an upper limit; these results are listed in Table 7. Then we determined the He II Zanstra temperature by the method given by Fernández-Castro et al. (1988), who use the ratio of the intensity of He II $\lambda$1640 to that of the continuum at $\lambda$1336, which they show is produced in the hot source only; they assume that the emitting region is optically thick to radiation shortward of the ionization limits of H and He II. This hypothesis may not be correct, and therefore this temperature must be considered as a lower limit to the effective temperature of the hot source. Since this last method requires UV observations, we have a lower limit only for 1995.

TABLE 7

UPPER LIMIT TO THE HOT COMPONENTS TEMPERATURE (in kelvins)

| Year | Hen 1341 | Hen 1761 |
|---|---|---|
| 1987..... | 148,000 | 136,000 |
| 1991..... | 144,000 | 94,000 |
| 1995..... | 154,000 | 142,000 |

### 6.2. *Radius and Luminosity of the Hot Sources*

Since we know the distance and the limiting values for the temperature, assuming that the hot source radiates as a blackbody, its limiting radii may be estimated by comparing the intensity of the radiation observed at $\lambda$1336 and the blackbody radiation emitted at the same wavelength, $\pi B_\lambda$:

$$L_\lambda = 4\pi d^2 I_\lambda = 4\pi R^2 \pi B_\lambda .$$

In theory, upper and lower limits of the luminosity may then be easily obtained from the relation

$$L = 4\pi R^2 \sigma T^4 .$$

TABLE 8

LIMITING PARAMETERS FOR THE HOT COMPONENTS

| HEN 1341 | | HEN 1761 | |
|---|---|---|---|
| $C\beta$(visual) | $C\beta$(UV) | $C\beta$(visual) | $C\beta$(UV) |
| 98,000 K $< T^* <$ 154,000 K | 108,000 K $< T^* <$ 151,000 K | 97,000 K $< T^* <$ 142,000 K | 102,000 K $< T^* <$ 140,000 K |
| $1.221 > R^*/R_\odot > 0.848$ | $0.104 > R^*/R_\odot > 0.081$ | $0.217 > R^*/R_\odot > 0.162$ | $0.056 > R^*/R_\odot > 0.044$ |
| $5.08 < \log (L^*/L_\odot) < 5.55$ | $3.11 < \log (L^*/L_\odot) < 3.48$ | $3.57 < \log (L^*/L_\odot) < 3.94$ | $2.47 < \log (L^*/L_\odot) < 2.81$ |

All these determinations depend strongly on $I(\lambda 1336)$, consequently the choice of the adequate value of the reddening constant is very important; thus we have made the calculations using both the visual and the UV-visual values of $C\beta$. The results are shown in Table 8, which is self-explanatory. We do not quote individual errors for each of the quantities listed, but from error transmission theory we find that the errors of the upper and lower limiting temperatures, and of the corresponding radii and luminosities, are of the order of 2%, 6%, 15%, and 50%–60%, respectively.

## 7. DISCUSSION

We have determined the reddening constant for Hen 1341 and Hen 1761, using the Balmer decrement method and the UV and visual He II lines. In both cases we have found strong differences between the two procedures, with the Balmer decrement values being larger than those given by the He II lines. The reason for these differences is not readily understood; one cause may be the existence of some errors associated with the calibration between the *IUE* results and the optical observations, but they should not be significant in comparison with the differences found here; other possibilities are that the reddening law applied is not adequate for the objects studied, or that the two reddening determinations are not really equal. Although in general UV and optical reddening determinations agree well, some differences have also been found by other authors. Vassiliadis et al. (1996), for example, presented spectroscopic observations of a group of planetary nebulae (for which no optical depth effects are to be expected) in the Magellanic Clouds, made with the *Hubble Space Telescope*; they find that, in general, the reddening determined from the He II $I(\lambda 1640)/I(\lambda 4686)$ emission-line ratio does not agree with that derived from the Balmer decrement, even though the difference of reddening functions between our Galaxy and the Magellanic Clouds was taken into account by the authors. As in our case, the UV reddening turns out to be smaller than the Balmer decrement reddening.

We have determined the optical depth at Hα, $\tau(\mathrm{H}\alpha)$, and the self-absorption correction factor for H($\beta$), Cs, for both objects and for each epoch of observation; the intensities corrected by the Balmer decrement reddenings have been used. To have a more significant set of data, we have introduced the results of the same calculations for several objects with observations presented in a previous paper (Gutiérrez-Moreno & Moreno 1996). We find that, as could be expected, both parameters are well correlated: taken as a whole, they define a linear relation, with a correlation coefficient $R = 0.951$. If the objects with more than one observation are analyzed separately, we find slopes that differ slightly for different objects.

As an experiment, we have plotted in Netzer's (1975) diagrams our observations of Hen 1341 and Hen 1761, corrected for reddening with reddening constants equal to 0.45 and 0.12, respectively; we find that the corresponding points agree better with the curves corresponding to $\tau(\mathrm{L}\alpha) = 10^4$–$10^5$ than to $10^6$, but with values of $\tau(\mathrm{H}\alpha)$ of the order of 50 or larger. Both $\tau(\mathrm{Ly}\alpha)$ and $\tau(\mathrm{H}\alpha)$ seem inadequate for our symbiotic stars, and we conclude that the optical values of $C\beta$ are more adequate, at least for the optical observations. On the other hand, a look at Table 8 shows that, in spite of the large errors, the limiting radii and luminosities of the hot sources seem more reasonable for the calculations made with the reddening obtained from the He II lines.

Both Hen 1341 and Hen 1761 show values of $\tau(\mathrm{H}\alpha)$ which are larger in 1987 than in 1991 and 1995; this is especially true for Hen 1761. The differences are larger than could be expected from the observational errors only, and suggest changes in the physical parameters $T_e$ or $N_e$ or in both simultaneously. Nevertheless, a look at Table 6 shows that the changes in both parameters seem too small to explain the variations found in $\tau(\mathrm{H}\alpha)$.

As can be seen in Tables 5 and 6, Hen 1341 shows a fairly constant behavior during the interval covered by the observations, except for the relative flux of Hα, which is larger in 1987 than in the other two periods. $N_e$ seems to have been increasing since 1987; this produces a diminution of the size of the nebula. The He content is rather high, similar to that of planetary nebulae of type I, and with a large fraction of $He^{++}$, which implies a large excitation. Table 7 does not show variations of the upper limit to the hot-component temperature.

Hen 1761 shows a very different behavior, with clear variations which are especially noticeable in 1991; during this period the object suffered some significant changes, mainly shown by the cooling of the hot component by about 33% (Table 7) and by an expansion of the nebula by a factor of the order of 2.5, without a significant change of the nebular temperature (Table 6). This implied a general enhancement of the emission as seen in Figure 5 and a diminution of the excitation shown by the smaller relative fluxes listed in Table 5. Besides, there is a diminution of the total nebular He content to about half the value of 1987—produced mainly by the change in the $He^{++}$ content—followed by an increase to a very high He abundance in 1995. This last result can be considered uncertain, since the value $\tau(\lambda 3889)$ used was arbitrary; nevertheless, for $\tau(\lambda 3889) = 0$ and 50, we get $y^+(\lambda 5876) = 0.227$ and 0.199, respectively, a change which is not significant with respect to the value listed in Table 6.

Hen 1761 seems to be losing matter steadily, through a wind detected both in He I and He II.

Table 8 shows that the limiting temperatures of the hot component do not change much with the reddening constant used. Within the errors of the observations, it may be considered that the two objects have the same limiting temperatures, independent of the reddening constant used. The changes become important for the radii and luminosities: considering these variations and the errors quoted in the preceding subsection, from Table 8, we can only conclude that the radii are larger than could be expected for white dwarfs and that during 1995 the hot component of Hen 1761 was smaller and less luminous than that of Hen 1341.

We are indebted to R. E. Williams and M. G. Smith of CTIO for the use of the Observatory facilities, and to the Visitors Support Group for their assistance during the observations. We thank Y. Kondo for making available Director's discretionary observing time at the *IUE*, and the *IUE* Observatory staff for making the observations under the Service Observing Program. We are grateful to J. García for his help with the 1991 observations, and to J. García and G. Valladares for their help at the CPDI of the Departamento de Astronomía de la Universidad de Chile. We also thank G. Cortés for her help in the handling of the data and of the manuscript. This work was partially supported by the Departamento Técnico de Investigación de la Universidad de Chile.

REFERENCES

Ahern, F. J. 1975, ApJ, 197, 639
Allen, D. A. 1982, in The Nature of Symbiotic Stars, ed. M. Friedjung & R. Viotti (Dordrecht: Reidel), 27
———. 1984, Proc. Astron. Soc. Australia, 5, 369
Almog, Y., & Netzer, H. 1989, MNRAS, 238, 57
Andrillat, Y. 1982, in The Nature of Symbiotic Stars, ed. M. Friedjung & R. Viotti (Dordrecht: Reidel), 47
Dyck, H. M., Lockwood, G. W., & Capps, R. W. 1974, ApJ, 189, 89
Feibelman, W. A. 1982, AJ, 87, 555
Feibelman, W. A., & Aller, L. H. 1987, ApJ, 319, 407
Fernández-Castro, T., Cassatella, A., Giménez, A., & Viotti, R. 1988, ApJ, 324, 1016
Gutiérrez-Moreno, A., & Moreno, H. 1996, PASP, 108, 972
Hamuy, M., Walker, A. R., Suntzeff, N. B., Gigoux, P., & Phillips, M. M. 1992, PASP, 104, 533
Iijima, T. 1981, in Photometric and Spectroscopic Binary Systems, ed. E. B. Carling & Z. Kopal (Dordrecht: Reidel), 517
*IRAS* Point Source Catalog, Version 2. 1988, Joint *IRAS* Science Working Group (Washington, DC: GPO)
Johnson, H. L. 1966, ARA&A, 4, 193
Kenyon, S. J. 1986, The Symbiotic Stars (Cambridge: Cambridge Univ. Press)
Kenyon, S. J., & Fernández-Castro, T. 1987, AJ, 93, 938
Meier, S. R., Kafatos, M., Fahey, R. P., & Michalitsianos, A. M. 1994, ApJS, 94, 183
Munari, U., Yudin, B. F., Taranova, O. G., Massone, G. F., Marang, F., Roberts, G., Winkler, H., & Whitelock, P. A. 1992, A&AS, 93, 383
Netzer, H. 1975, MNRAS, 171, 395
Nussbaumer, H., & Storey, P. J. 1981, A&A, 99, 177
Savage, B. D., & Mathis, J. S. 1979, ARA&A, 17, 73
Schmid, H. M. 1989, A&A, 211, L31
Seaton, M. J. 1979, MNRAS, 187, 73P
Stone, R. P. S., & Baldwin, J. A. 1983, MNRAS, 204, 347
Taylor, B. J. 1984, ApJS, 54, 259
Tsuji, T. 1978, A&A, 62, 29
Turnshek, D. E., Turnshek, D. A., Craine, E. R., & Boeshaar, P. C. 1985, An Atlas of Digital Spectra of Cool Stars (Tucson: Western Research Co.)
Vassiliadis, E., Dopita, M. A., Bohlin, R. C., Harrington, J. P., Ford, H. C., Meatheringham, S. J., Wood, P. R., Stecher, T. P., & Maran, S. P. 1996, ApJS, 105, 375